

Nonlinear magnetotransport in Weyl semimetal

Debottam Mandal,^{*} Kamal Das,[†] and Amit Agarwal[‡]

Department of Physics, Indian Institute of Technology Kanpur, Kanpur 208016

The recent discovery of the quantum nonlinear Hall effect has revived the field of nonlinear transport. Here, we predict magnetic field induced nonlinear Hall effect in time reversal symmetric Weyl semimetal. We show that the interplay of the band geometric quantities, such as the Berry curvature, and the magnetic part of the Lorentz force can give rise to finite nonlinear Hall conductivity that is linear in the magnetic field. Such nonlinear Hall conductivity can manifest through nonlinear transport measurement as well as nonlinear optical phenomena like photocurrent and the second harmonic generation.

I. INTRODUCTION

Weyl semimetals (WSM) are well known for hosting low energy quasi-particle excitation which mimic the properties of Weyl fermions [1–8]. Their novel bulk electronic structure comprises of doubly degenerate linear band crossing of non-degenerate bands, known as Weyl nodes. In addition, these materials support non-trivial and exotic Fermi arc states on their surface. Intense research focused on the impact of Weyl quasi-particles on physical properties has led to the discovery of several novel bulk phenomena [9] such as the quantum anomalies [10], and some unconventional surface phenomena [11 and 12]. Many of the bulk properties of WSM can be understood in terms of the Berry curvature associated with Weyl nodes, which act as source and sink of Berry curvature depending on the chirality of the nodes. The Weyl semimetal phase with space inversion symmetry (SIS) is realized in some magnetic systems [1, 13, and 14], and it can also be induced in Dirac semimetals such as Cd₃As₂ [15], and Na₃Bi [16] by a magnetic field. Weyl systems with time reversal symmetry (TRS) have been realized in the TaAs family [2–4, and 17], amongst others. In addition to these, WSM where both the symmetries are broken [18] have been recently realized in RAlGe family (R = rare-earth) [19] and in CeAlSi [20].

The realization of WSM in SIS broken materials has further promoted the exploration of second order nonlinear (NL) responses [21–23] in them. It has been shown that due to its topological aspects, the photogalvanic responses [24–31] and the second harmonic generation [32] show novel behaviour in WSM. Furthermore, the recently discovered Berry curvature dipole induced NL anomalous Hall effect [33–38] has also been realized in WSM [39–41] in the absence of any magnetic field. Owing to these, it is expected that the NL responses of WSM in the presence of a magnetic field will also incorporate rich physics [42–44]. In the strong magnetic field limit, the NL conductivities have been found to show quantum oscillation behavior [26 and 28] owing to the presence of Landau levels, while the Berry curvature induced corrections in the semiclassical equation of motion [45], has been shown to give rise to non-trivial responses in the weak magnetic field regime [42, 43, 46–50].

Here, we predict a new magnetic field induced NL Hall

effect in WSM with time reversal symmetry. Using the semiclassical Boltzmann transport formalism in the weak magnetic field regime, we show that the SIS broken WSM possesses NL Hall conductivities that vary linearly with the magnetic field. These arise from the interplay between the band geometric quantities, and the magnetic field component of the Lorentz force.

More specifically, we show that the NL Hall conductivity with the same last two indices can be expressed as $\sigma_{abb} \propto B_a \delta_{\hat{a} \times \hat{b}, \hat{c}}$, where a, b, c are the orthogonal Cartesian coordinates. Such NL Hall conductivity (perpendicular to the applied electric field) drives current along the direction of the magnetic field. The physical mechanisms responsible for this are the Lorentz force, the Berry curvature dependent correction to the phase-space factor and the Berry curvature induced magnetic velocity correction. Furthermore, the NL Hall conductivity with the different last two indices can be expressed as $\sigma_{aab} \propto B_b$. For such NL conductivities current flows perpendicular to the direction of the magnetic field. The mechanism behind this contribution are the Lorentz force, correction to the phase-space factor and the ‘Berry force’. These novel NL Hall conductivity can be measured through NL resistivity measurements in magneto-transport experiments [51–54]. In addition they can also manifest through nonlinear optical experiment of photocurrent and second harmonic generation.

The rest of the paper is organised as follows: In Sec. II we discuss the semiclassical Boltzmann transport formalism and derive the generic forms of the NL conductivities. We present our model specific calculations of the NL conductivities for the inversion symmetry broken WSM in Sec. III. Finally we summarize our results in Sec. IV.

II. SEMICLASSICAL THEORY FOR NONLINEAR CONDUCTIVITIES

In this section, we present the general expressions of second order NL conductivities in quantum materials in presence of a magnetic field. For an AC electric field, two different NL conductivities are commonly defined. The second harmonic conductivity relates the applied electric field to the second harmonic current [$j_2^{(2\omega)}$] via the phenomenological relation $j_{2,a}^{(2\omega)} = \sigma_{abc} E_b E_c$. Here, sum over

the repeated spatial indices (a, b, c) is implied. The DC or rectification NL conductivity (σ_{abc}^R) relates the rectification current $[j_2^{(0)}]$ to the applied electric field through $j_{2,a}^{(0)} = \sigma_{abc}^R E_b E_c^*$. In this work we primarily focus on the second harmonic conductivity.

To calculate the NL current, we employ the semi-classical Boltzmann transport formalism. In this formalism, the electrical current is expressed as $\mathbf{j} = -e \int [d\mathbf{k}] D^{-1} \hat{\mathbf{r}} g(t)$, where ‘ $-e$ ’ is the electronic charge and $[d\mathbf{k}] = d\mathbf{k}/(2\pi)^3$. It is evident from the above expression that we need three key ingredients for calculating the current. These are *i*) the equations of motion of the carriers, *ii*) the phase-space density D^{-1} and, *iii*) the non-equilibrium distribution function (NDF) $g(t)$.

In presence of a homogeneous time dependent electric field $\mathbf{E}(t)$ and a static magnetic field \mathbf{B} , the equations of motion of the charge carriers, in a given band are given by [55–58]

$$\dot{\mathbf{r}} = D \left[\tilde{\mathbf{v}} + \frac{e}{\hbar} \mathbf{E} \times \boldsymbol{\Omega} + \eta \frac{e}{\hbar} (\tilde{\mathbf{v}} \cdot \boldsymbol{\Omega}) \mathbf{B} \right], \quad (1)$$

$$\hbar \dot{\mathbf{k}} = D \left[-e \mathbf{E} - \alpha e (\tilde{\mathbf{v}} \times \mathbf{B}) - \zeta \frac{e^2}{\hbar} (\mathbf{E} \cdot \mathbf{B}) \boldsymbol{\Omega} \right]. \quad (2)$$

Here, $1/D = [1 + \gamma \frac{e}{\hbar} \mathbf{B} \cdot \boldsymbol{\Omega}]$ is the phase-space factor and $\boldsymbol{\Omega} = \nabla_{\mathbf{k}} \times \langle u | i \nabla_{\mathbf{k}} | u \rangle$ is the Berry curvature with $|u\rangle$ being the periodic part of the Bloch wave-function. The band velocity, modified by the orbital magnetic moment (OMM) \mathbf{m} , is given by $\tilde{\mathbf{v}} = \mathbf{v} - \mathbf{v}_m$ where we have defined $\hbar \mathbf{v} = \partial \epsilon / \partial \mathbf{k}$ and $\hbar \mathbf{v}_m = \partial \epsilon_m / \partial \mathbf{k}$ with $\epsilon_m = \mathbf{m} \cdot \mathbf{B}$. Note that the magnetic field modifies the band energy as $\tilde{\epsilon} = \epsilon - \xi \epsilon_m$, through the Zeeman like coupling of the magnetic field and the OMM, $\mathbf{m} = -i \frac{e}{2\hbar} \langle \nabla_{\mathbf{k}} u | \times (\hat{H} - \epsilon) | \nabla_{\mathbf{k}} u \rangle$. We emphasize that to keep track of the sources of various magnetic field dependences, we explicitly put α for the magnetic part of the Lorentz force, ζ for the ‘Berry force’, η for the magnetic velocity, γ for the phase-space factor and ξ for the OMM. At the end of the calculation, all these ‘tracking’ factors will be set to 1.

The NDF is calculated from the iterative solutions of the Boltzmann equation within the relaxation time approximation. It is given by [59]

$$\frac{\partial g(t)}{\partial t} + \dot{\mathbf{k}} \cdot \nabla_{\mathbf{k}} g(t) = -\frac{g(t) - \tilde{f}}{\tau}. \quad (3)$$

Here, $\tilde{f} = f(\epsilon - \xi \mathbf{m} \cdot \mathbf{B})$ with $f(\epsilon) = 1/[e^{(\epsilon - \mu)/k_B T}]$ being the equilibrium Fermi-Dirac distribution function at chemical potential μ and temperature T with k_B being the Boltzmann constant. In Eq. (3), τ is the relaxation time whose energy dependence is ignored for simplicity.

In the weak electric field limit, the non-equilibrium part of the distribution function can be written as a power series of electric field dependent terms: $\sum_{n=1}^{\infty} f_n$ where $f_n \propto E^n$. We restrict ourselves upto f_2 for the calculation of second order NL response. Accordingly, we consider the ansatz [33 and 60]

$$f_2(t) = f_2^{(0)} + f_2^{(0)*} + f_2^{(2\omega)} e^{i2\omega t} + f_2^{(2\omega)*} e^{-i2\omega t}, \quad (4)$$

where $f_2^{(0)}$ represents the DC (or rectification) part and $f_2^{(2\omega)}$ represents the second harmonic part of the NL distribution function. Substituting the ansatz of Eq. (4) into Eq. (3) and following the usual Zener-Jones method [61], we obtain

$$f_2^{(2\omega)} = \sum_{\nu=0}^{\infty} \left(\alpha D \tau_{2\omega} \hat{L} \right)^{\nu} D \frac{e \tau_{2\omega}}{\hbar} \left(\mathbf{E} + \zeta \frac{e}{\hbar} (\mathbf{E} \cdot \mathbf{B}) \boldsymbol{\Omega} \right) \cdot \nabla_{\mathbf{k}} f_1^{(\omega)}. \quad (5)$$

Here, $f_1^{(\omega)}$ is the first order in electric field contribution of the NDF [see Appendix A for details]. We have defined $\hat{L} = \frac{e}{\hbar} (\mathbf{v} \times \mathbf{B}) \cdot \nabla_{\mathbf{k}}$ as the Lorentz force (magnetic part) operator. The modified scattering times are defined as $\tau_{\omega} = \tau/(1+i\omega\tau)$ and $\tau_{2\omega} = \tau/(1+i2\omega\tau)$. It is straightforward to expand the master solution, Eq. (5), and obtain the distribution function up to any order of magnetic field dependence. In this paper we are interested in the lowest (linear) order of magnetic field dependence and the key steps of the calculation have been highlighted in Appendix B. Note that from Eq. (5) we can construct the rectification part of the distribution function $f_2^{(0)}$ by substituting $\tau_{2\omega} \rightarrow \tau$ and $\mathbf{E} \rightarrow \mathbf{E}^*$.

Using the calculated NDF, we now calculate the NL conductivities. We emphasize that in addition to the second order NL distribution function, the NL current can also arise from linear- \mathbf{E} part of the distribution function when it is combined with the anomalous velocity $\mathbf{E} \times \boldsymbol{\Omega}$. The NL conductivities can be expressed in the form of a momentum dependent conductivity, $\tilde{\sigma}_{abc}$, where $\sigma_{abc} = -e^3 \tau_{\omega} / \hbar \int [d\mathbf{k}] \tilde{\sigma}_{abc}$. The magnetic field independent part of the NL conductivity is obtained to be

$$\tilde{\sigma}_{abc}^{(0)} = \varepsilon_{abd} \Omega_d v_c f' + \tau_{2\omega} v_a \partial_b v_c f'. \quad (6)$$

Here, ε_{abd} is the anti-symmetric Levi-civita symbol and $f' \equiv \partial_{\epsilon} f$. The first term of Eq. (6) is the NL anomalous Hall conductivity [35] and the second term is the NL Drude conductivity. The expression of magnetic field dependent part of the NL conductivity is a bit more complicated as various magnetic field contributions come into play. The total NL conductivity (linear in the magnetic field) can be expressed as $\tilde{\sigma}_{abc}^{(1)} = \tilde{\sigma}_{abc}^{(\eta)} + \tilde{\sigma}_{abc}^{(\zeta)} + \tilde{\sigma}_{abc}^{(\alpha)} + \tilde{\sigma}_{abc}^{(\gamma)} + \tilde{\sigma}_{abc}^{(\xi)}$. The different contributions to the magneto-conductivity can be calculated to be

$$\tilde{\sigma}_{abc}^{(\eta)} = \tau_{2\omega} \Omega_{\nu} B_a \partial_b v_c f', \quad (7)$$

$$\tilde{\sigma}_{abc}^{(\zeta)} = \varepsilon_{abd} \Omega_d \Omega_{\nu} B_c f' + \tau_{2\omega} v_a (\Omega_B^{\text{db}} \partial_d v_c + B_c \partial_b \Omega_{\nu}) f', \quad (8)$$

$$\tilde{\sigma}_{abc}^{(\alpha)} = \tau_{\omega} \varepsilon_{abd} \Omega_d \hat{L} v_c f' + v_a (\tau_{2\omega}^2 \hat{L} \partial_b + \tau_{\omega} \tau_{2\omega} \partial_b \hat{L}) v_c f', \quad (9)$$

$$\tilde{\sigma}_{abc}^{(\gamma)} = -\varepsilon_{abd} \Omega_d \Omega_B v_c f' - \tau_{2\omega} v_a (\Omega_B \partial_b + \partial_b \Omega_B) v_c f', \quad (10)$$

$$\tilde{\sigma}_{abc}^{(\xi)} = -\varepsilon_{abd} \Omega_d (v_{mc} f' + \epsilon_m v_c f'') - \tau_{2\omega} v_{ma} \partial_b v_c f' - \tau_{2\omega} v_a \partial_b (v_{mc} f' + \epsilon_m v_c f''). \quad (11)$$

Here, we have defined $\Omega_B^{\text{db}} \equiv (e/\hbar) \Omega_d B_b$ and $\Omega_{\nu} \equiv (e/\hbar) \boldsymbol{\Omega} \cdot \mathbf{v}$ and $f'' \equiv \partial_{\epsilon}^2 f$. We emphasize here that the

derivative operator $\partial_b = \partial/\partial k_b$ and \hat{L} operate on all the terms appearing to their right hand side. Together, Eqs. (7)-(11) describe all the NL conductivity components, which vary linearly with the magnetic field.

In materials which preserve SIS, the energy dispersion, Berry curvature and the OMM are even functions of the crystal momentum. Consequently, the orbital magnetic moment coupling energy and the corresponding velocity satisfy $\epsilon_m(-\mathbf{k}) = \epsilon_m(\mathbf{k})$ and $\mathbf{v}_m(-\mathbf{k}) = -\mathbf{v}_m(\mathbf{k})$ respectively, and the bare band velocity obeys $\mathbf{v}(-\mathbf{k}) = -\mathbf{v}(\mathbf{k})$. Using these conditions, it is straightforward to show that all the NL conductivities [Eqs. (6)-(11)] vanish in presence of SIS, as expected. If the SIS is broken, the presence or absence of TRS affects the NL conductivity. In presence of TRS, while the energy dispersion is an even function, the Berry curvature and the OMM are odd functions of the crystal momentum. Consequently we have $\epsilon_m(-\mathbf{k}) = -\epsilon_m(\mathbf{k})$, $\mathbf{v}_m(-\mathbf{k}) = \mathbf{v}_m(\mathbf{k})$ and $\mathbf{v}(-\mathbf{k}) = -\mathbf{v}(\mathbf{k})$. Within these constraints, we find that for the magnetic field independent NL conductivities ($\sigma_{abc}^{(0)}$), contributions that are quadratic in the scattering time vanish while linear scattering time dependent contributions are finite. On the other hand, for linear magnetic field dependent NL conductivity ($\sigma_{abc}^{(1)}$), contributions that are quadratic in scattering time survive while the other (linear and cubic) scattering time dependent contributions vanish.

For completeness, and to complement the discussion of the NL conductivity, we also discuss the linear conductivity of WSM [see Appendix A for detailed derivation]. The magnetic field independent linear conductivity is given by

$$\sigma_{ab}^{(0)} = -e^2\tau_\omega \int [d\mathbf{k}] v_a v_b f' - \frac{e^2}{\hbar} \varepsilon_{abc} \int [d\mathbf{k}] \Omega_c f. \quad (12)$$

Here, the first term is the Drude conductivity and the second term is the intrinsic anomalous Hall conductivity which vanishes in TRS invariant systems. The linear order in magnetic field contribution to the linear conductivity is given by,

$$\begin{aligned} \sigma_{ab}^{(1)} = & -e^2\tau_\omega \int [d\mathbf{k}] \left[(\eta\Omega_v B_a v_b + \alpha\tau_\omega v_a \hat{L} v_b \right. \\ & - \gamma v_a \Omega_B v_b + \zeta v_a \Omega_v B_b) f' - \xi \left\{ (v_m a v_b \right. \\ & \left. \left. + \hbar^{-1} \tau_\omega^{-1} \varepsilon_{abd} \Omega_d \epsilon_m + v_a v_m b) f' + v_a \epsilon_m v_b f'' \right\} \right]. \end{aligned} \quad (13)$$

It can be easily checked that in a TRS invariant system, the diagonal components ($a = b$) of Eq. (13) will vanish, consistent with Onsager's relation. So we can only have the linear- \mathbf{B} dependent Hall components ($a \neq b$). Furthermore, we find that in presence TRS only those contributions to the linear- \mathbf{B} conductivity are nonzero which are quadratic and zeroth order in the scattering time. From Eq. (13) it is evident that the quadratic dependence of scattering time is described by the Lorentz force and the scattering time independent contribution has its origin in the OMM [62].

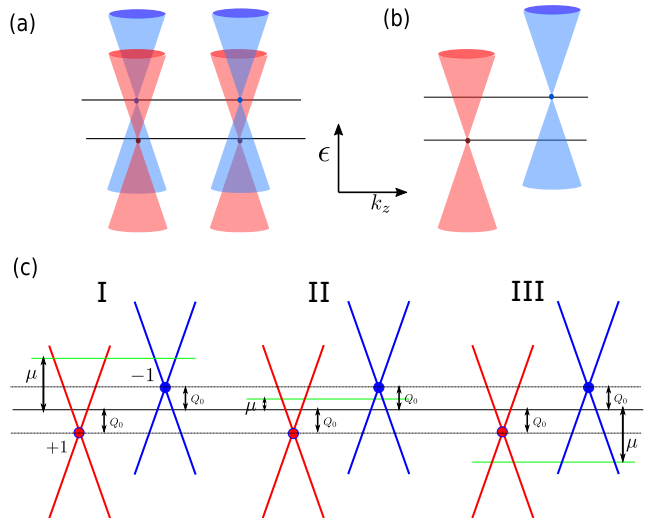


FIG. 1. A schematic depiction of the band dispersion for a) TRS preserving and SIS broken WSM, and b) TRS broken (with SIS preserved) WSM. Due to the presence of TRS, minimum four Weyl nodes are required in the SIS broken WSM. In contrast, when TRS is absent and SIS is present, a minimum two Weyl nodes is possible. (c) shows three different scenarios for the location of the Fermi level, with respect to the location of the Weyl points. In the left panel the Fermi level is in the conduction band of both Weyl nodes ($\mu > Q_0 > 0$). In the middle panel the Fermi energy lies in the conduction band of one Weyl node and in the valence band of the other Weyl node ($Q_0 > \mu > -Q_0$). The right panel shows the scenario when the Fermi level lies in the valence band of both the Weyl nodes ($\mu < -Q_0 < 0$).

The framework presented in this section for exploring the NL magneto-conductivity is very general, and applicable to all SIS broken materials. In the rest of the paper, we apply this to explore the NL magneto-conductivity in time reversal symmetric WSM.

III. NONLINEAR CONDUCTIVITY IN WEYL SEMIMETAL

In this section, we calculate the linear and NL magneto-conductivity for an SIS broken WSM. The simultaneous presence of TRS and SIS forces all the bands in the given material to be doubly degenerate, and this excludes the possibility of the formation of a WSM, in which two non-degenerate linearly dispersing bands cross each other [8]. Thus, for realizing a WSM state, either SIS or TRS or both the symmetries must be broken. In a TRS preserving (SIS broken) WSM, a minimum of four Weyl nodes [63–65] have to be there. Among the four nodes, the nodes with the same chirality are connected by a time reversal invariant momentum and corresponding charge neutrality points reside at the same energy.

However, there are no symmetry restriction among the nodes with different chirality. On the other hand, in a SIS preserving (TRS broken) WSM, a minimum of a single pair of two Weyl nodes of opposite chirality are allowed, and for each such pair of Weyl nodes, the corresponding charge neutrality point reside at different energies. Both of these scenarios have been sketched in Fig. 1(a)-(b) respectively. In our work, we present the NL conductivity calculation for a TRS invariant WSM with minimum four Weyl nodes shown in Fig. 1(a).

The low energy Hamiltonian of a single Weyl node can be written as [18, 66–69]

$$H_s(\mathbf{k}) = s\hbar v_F \boldsymbol{\sigma} \cdot (\mathbf{k} - s\mathbf{Q}) - sQ_0. \quad (14)$$

Here, \mathbf{k} is the crystal momentum, $\boldsymbol{\sigma} = (\sigma_x, \sigma_y, \sigma_z)$ are the Pauli matrices, v_F is the Fermi velocity and $s = \pm 1$ is the chirality index. In Eq. (14), the \mathbf{Q} and Q_0 denotes the position of the Weyl nodes in the momentum and energy, respectively. For simplicity of calculation, we consider the case where the Weyl node is situated at the origin and emphasize that non-zero \mathbf{Q} , which breaks the time reversal symmetry, does not alter any of the results. With $\mathbf{Q} = 0$, the Hamiltonian in Eq. (14) simplifies to, $H_s(\mathbf{k}) = s\hbar v_F \boldsymbol{\sigma} \cdot \mathbf{k} - sQ_0$. The breaking of SIS in this model is reflected through the finite Q_0 which positions the Weyl nodes of opposite chirality at different energy. More specifically, the Weyl point of the positive chirality node lie at energy $-Q_0$ while the Weyl point for the negative chirality node lies at Q_0 , making the energy separation between the two Weyl nodes to be $2Q_0$. On the other hand, the TRS is enforced here by considering a minimum of four Weyl nodes in such a way that the two nodes of same chirality out of the four are situated at the same energy [see Fig. 1(a)]. The energy dispersion and band velocity for the Hamiltonian are given by $\epsilon_s(\mathbf{k}) = s_b \hbar v_F k - sQ_0$ and $\mathbf{v}(\mathbf{k}) = s_b v_F \mathbf{k}/k$ respectively, where $k = |\mathbf{k}|$ and $s_b = +1(-1)$ for the conduction (valence) band. We note that non-zero Q_0 makes $\epsilon_+(\mathbf{k}) \neq \epsilon_-(\mathbf{k})$, implying the breaking of inversion symmetry. The Berry curvature and the OMM for this model are given by [43 and 50]

$$\boldsymbol{\Omega} = -s s_b \frac{\mathbf{k}}{2k^3}; \quad \mathbf{m} = -s e v_F \frac{\mathbf{k}}{2k^2}, \quad (15)$$

respectively. We note that these band geometric quantities do not depend on the energy separation (Q_0) of the Weyl points in the corresponding Weyl nodes. In contrast to the Berry curvature, the OMM is independent of the band index. Both these band geometric quantities are highly concentrated near the Weyl point, as expected.

Using these in Eqs. (6)-(11), we calculate the NL conductivity and the symmetrized results $\bar{\sigma}_{abc} = (\sigma_{abc} + \sigma_{acb})/2$ are summarized in Table I. We note that the NL Drude conductivity is identically zero due to the presence of TRS. Furthermore, we find that the NL anomalous Hall conductivity is also zero. Although individual Weyl node possesses finite NL anomalous Hall conductivity, the total response vanishes after summing over the

nodes. This happens due to the absence of Berry curvature dipole in this system. In order to realize the NL anomalous response [35], the mirror symmetry has to be broken. This is generally achieved in WSM with tilt or with higher order (band bending) terms [35, 38, 70, and 71] in the effective Hamiltonian.

Coming to the linear magnetic field dependent NL conductivities, all the conductivities and their origin of magnetic field dependences are explicitly highlighted in Table I. For compactness, the various components of the conductivity are expressed as $\bar{\sigma}_{abc} = \tilde{\sigma}_{\text{NL}} B_d(\eta, \alpha, \gamma, \zeta, \xi)$ where B_d is the component of the magnetic field along the $d \in (x, y, z)$ axis, and the total contribution is given by the sum of different magnetic field sources. We have defined

$$\tilde{\sigma}_{\text{NL}} = \frac{e^4 v_F^2 \tau^2}{\pi^2 \hbar^2 |\mu|} \frac{r_0}{3(1-r_0^2)}, \quad (16)$$

with $r_0 \equiv Q_0/|\mu|$. We find three key features in the NL conductivities. i) All the longitudinal NL conductivities (σ_{aaa}) vanish within the linear- \mathbf{B} approximation. ii) We find that the NL Hall components with the same last two indices, which we term as ‘pure’ Hall components, such as $\bar{\sigma}_{zxx}, \bar{\sigma}_{yzz}, \bar{\sigma}_{xyy}$ are non-zero and determined by the magnetic velocity term (η) in addition to the phase-space factor (γ) and the magnetic part of the Lorentz force (α). These NL conductivities can be expressed as $\sigma_{abb} \propto B_a \delta_{\hat{\mathbf{a}} \times \hat{\mathbf{b}}, \hat{\mathbf{c}}}$ which implies that the currents corresponding to the conductivity flow along the direction of the applied magnetic field. iii) The NL Hall components with different the last two indices, which we term as the ‘mixed’ Hall components, are determined by the Berry force (ζ) in addition to the phase-space factor (γ) and the Lorentz force (α). The magnetic field dependence of the mixed components, $\sigma_{aab} \propto B_b$, implies that the currents corresponding to the conductivity flow perpendicular to the magnetic field direction. These are the main findings of our paper in the context of SIS broken WSM. Interestingly, we find that the OMM (ξ) contributions to the NL conductivity is identically zero for the TRS preserving case.

We emphasize here that for the calculation of conductivities for Weyl nodes with opposite chirality separated in energy, three different scenarios based on the position of the Fermi level as highlighted in Fig. 1(c), are possible. In scenario-I, the Fermi level resides in the conduction band of both the Weyl nodes. In scenario-II, the Fermi level resides in the conduction band of one Weyl node and in the valence band of the other Weyl node. In scenario-III, the Fermi level resides in the valence band of both the Weyl nodes. Interestingly, we find that the total conductivity, including all the Weyl nodes, can be expressed by same expression for these three scenarios. This has been shown in Appendix C in detail.

Although we have considered the three scenarios, a continuous transition of Fermi level among them is not allowed within our formalism. This is due to the fact that the employed semiclassical Boltzmann formalism is gen-

TABLE I. Symmetrized nonlinear conductivity $\bar{\sigma}_{abc}$ in the unit of $\tilde{\sigma}_{\text{NL}}$, which is defined in Eq. (16), for the TRS invariant WSM. The Greek indices in the parentheses denote the sources of the magnetic field that are inducing finite conductivity and the total is obtained by adding all the contributions. The diagonal components of the NL conductivity are identically zero. The NL Hall conductivities with same last two indices (σ_{abb}) are non-zero when a and b are cyclic coordinates and the magnetic field dependence is dictated by B_a . The Hall conductivities with different last two indices can be written as $\bar{\sigma}_{aab} = \bar{\sigma}_{aba}$ and its magnetic field dependence is determined by B_b .

$\bar{\sigma}_{abc}$	$\bar{\sigma}_{aax}$	$\bar{\sigma}_{aay}$	$\bar{\sigma}_{aaz}$	$\bar{\sigma}_{axy}$	$\bar{\sigma}_{ayz}$	$\bar{\sigma}_{azz}$
$\bar{\sigma}_{xbc}$	0	$B_x(2\eta + \alpha - \gamma)$	0	$-B_y(\frac{\alpha}{2} - \frac{\gamma}{2} + \zeta)$	0	0
$\bar{\sigma}_{ybc}$	0	0	$B_y(2\eta + \alpha - \gamma)$	0	$-B_z(\frac{\alpha}{2} - \frac{\gamma}{2} + \zeta)$	0
$\bar{\sigma}_{zbc}$	$B_z(2\eta + \alpha - \gamma)$	0	0	0	0	$-B_x(\frac{\alpha}{2} - \frac{\gamma}{2} + \zeta)$

erally valid at high carrier densities such that $\mu \gg \hbar/\tau$ [59]. Hence, the above results are not applicable near the limit $|r_0| = 1$, where the chemical potential is located at the Weyl point of either of the two Weyl nodes.

Now, we compare our results with some recent related works [43 and 50] and highlight the differences. We note that in Ref. [43] the authors provide result of a single Weyl node. To our satisfaction, we can obtain those results by putting $Q_0 = 0$ in our single node calculations presented in Appendix C. We emphasize that total NL responses from all nodes are zero for $Q_0 = 0$ as the inversion symmetry is restored. Recently in Ref. [50], it has been shown that the inversion symmetry broken tilted WSM possesses NL magnetoresponse. We note that the NL conductivities discussed in Ref. [50] are linear in scattering time, τ , however the NL conductivities we discuss in our paper are proportional to the square of the scattering time, τ^2 . We emphasize here that the TRS has to be broken in addition to SIS in order to obtain linear- τ dependent NL magneto-conductivity. Comparing the order of magnitude of NL conductivities discussed in our paper with the results in Ref. [50] we find that for certain parameter values $v_F = 3 \times 10^5$ m/s, $\tau = 10^{-13}$ s, $R_s(\text{tilt}) = 0.5$, $\mu = 20$ meV and $Q_0 = 10$ meV, the conductivities are of the comparable order: $\sigma(R_s = 0)/\sigma(R_s \neq 0) \sim \mathcal{O}(10^1)$, where $\sigma(R_s = 0) = \tilde{\sigma}_{\text{NL}}$ and $\sigma(R_s \neq 0)$ is the NL conductivity in Eq. (11) of [50].

For completeness, we now discuss the linear conductivity of WSM, starting from Eqs. (12)-(13). As expected from the Onsager relations, the magnetic field induced part of the longitudinal components are identically zero and the Drude conductivity is obtained to be [68]

$$\sigma_{aa} = \frac{2e^2\tau\mu^2(1+r_0^2)}{3\pi^2\hbar^3v_F}, \quad (17)$$

where $a = (x, y, z)$. The Drude contribution is linear in the scattering time and quadratic in the node separation. The Drude conductivity in Eq (17) reduces to the known result [68 and 72] in the limit of zero energy separation between the Weyl points, $Q_0 = 0$. Here, the modification in the Drude conductivity corresponds to the fact that the energy separation between the nodes gives rise to different carrier concentrations at the opposite chirality.

The linear Hall conductivity is given by

$$\sigma_{ab} = -\varepsilon_{abc}B_c \frac{e^3v_F\mu}{6\pi^2\hbar^3} \left(\xi \frac{\hbar^2}{\mu^2(1-r_0^2)} + 4\alpha\tau^2 \right). \quad (18)$$

We highlight that the Hall conductivity has two components, one is quadratic and the other is zeroth order in the scattering time. While the former extrinsic contribution has its origin in the Lorentz force (term $\propto \alpha$), the latter intrinsic contribution (term $\propto \xi$) originates from the OMM [62].

IV. SUMMARY AND CONCLUSION

To wrap up, in this paper we have investigated the second order NL conductivity in time reversal symmetric WSM in presence of a weak magnetic field. Starting from the semiclassical Boltzmann transport formalism, we obtain the general expressions of all the NL Hall conductivities, and identify the different physical mechanisms contributing to the magnetic field dependencies. Using the developed framework for NL magneto-conductivity in conjugation with appropriate symmetry analysis, we calculate the NL Hall conductivity in WSM without any tilt. Our calculations explicitly highlight the interplay of the quantum geometric Berry curvature and the magnetic part of the Lorentz force. We predict two types of new NL Hall effects. In one case, which we term as pure NL Hall effect, the current flows along the direction of the magnetic field, but perpendicular to the applied electric field. In the other case, which we term as the mixed NL Hall effect, the NL current flows perpendicular to the magnetic field direction. These newly predicted NL conductivity in WSM can be probed through NL magneto-transport or through NL magneto-optical experiments.

V. ACKNOWLEDGMENTS

We acknowledge Department of Physics, IIT Kanpur, the Science Education and Research Board (SERB) and the Department of Science and Technology (DST), Government of India.

Appendix A: Semiclassical theory for linear conductivities

In this section of Appendix, we will calculate current that is linear in \mathbf{E} -field and linear in \mathbf{B} -field. We assume that in the steady state the first order distribution function oscillates with fundamental frequency with the form [33 and 43] $f_1(t) = f_1^{(\omega)} e^{i\omega t} + f_1^{(\omega)*} e^{-i\omega t}$. Using this ansatz in the Boltzmann equation, Eq. (3), we obtain

$$f_1^{(\omega)} = \sum_{\nu} \left(\alpha D \tau_{\omega} \hat{L} \right)^{\nu} D \frac{e\tau_{\omega}}{\hbar} \left[\mathbf{E} + \zeta \frac{e}{\hbar} (\mathbf{E} \cdot \mathbf{B}) \boldsymbol{\Omega} \right] \cdot \nabla_{\mathbf{k}} \tilde{f}. \quad (\text{A1})$$

We expand the series in Eq. (A1) in orders of \mathbf{B} -field in the limit of small magnetic field [42, 45, and 61]. Using this expansion, the non-equilibrium part can be written as $f_1^{(\omega)} = f_{10}^{(\omega)} + f_{11}^{(\omega)}$, where the first subscript denotes the order of electric field and the second subscript denotes the order of magnetic field. We obtain

$$f_{10}^{(\omega)} = e\tau_{\omega} \mathbf{E} \cdot \mathbf{v} f', \quad (\text{A2})$$

$$f_{11}^{(\omega)} = e\tau_{\omega} (\zeta \Omega_{\nu} \mathbf{B} - \gamma \Omega_{\text{B}} \mathbf{v}) \cdot \mathbf{E} f' - \xi e\tau_{\omega} \mathbf{E} \cdot (\mathbf{v}_{\text{m}} f' + \epsilon_{\text{m}} \mathbf{v} f'') + \alpha e\tau_{\omega}^2 \hat{L} \mathbf{v} \cdot \mathbf{E} f'. \quad (\text{A3})$$

We note that these results are consistent with the previous studies [42, 43, 45, and 73].

Using the distribution functions we can calculate current. The zeroth order in \mathbf{B} -field current can be written as $\mathbf{j}_{10}(t) = \mathbf{j}_{10}^{(\omega)} e^{i\omega t} + \mathbf{j}_{10}^{(\omega)*} e^{-i\omega t}$. Separating the different order of scattering time dependence, we obtain

$$\mathbf{j}_{10}^{(\omega)}(\tau_{\omega}^0) = -\frac{e^2}{\hbar} \int [d\mathbf{k}] (\mathbf{E} \times \boldsymbol{\Omega}) f, \quad (\text{A4})$$

$$\mathbf{j}_{10}^{(\omega)}(\tau_{\omega}) = -e^2 \tau_{\omega} \int [d\mathbf{k}] \mathbf{v} (\mathbf{E} \cdot \mathbf{v}) f'. \quad (\text{A5})$$

The first one is the intrinsic anomalous Hall effect where current flows perpendicular to the electric field. Symmetry analysis shows that in presence of TRS, the anomalous Hall effect vanishes. The second one is the ordinary Drude current. The linear order in \mathbf{B} -field current can be written as $\mathbf{j}_{11}(t) = \mathbf{j}_{11}^{(\omega)} e^{i\omega t} + \mathbf{j}_{11}^{(\omega)*} e^{-i\omega t}$. We emphasize that ‘equilibrium’ distribution function in presence of a magnetic field, $\tilde{f} = f - \xi \epsilon_{\text{m}} f'$ also contributes to the current in addition to the non-equilibrium parts Eqs. (A2)-(A3). Now, using these we calculate current in various order in scattering time. The

even power of scattering time dependent current is given by

$$\mathbf{j}_{11}^{(\omega)}(\tau_{\omega}^0) = \frac{e^2}{\hbar} \xi \int [d\mathbf{k}] (\mathbf{E} \times \boldsymbol{\Omega}) \epsilon_{\text{m}} f', \quad (\text{A6})$$

$$\mathbf{j}_{11}^{(\omega)}(\tau_{\omega}^2) = -e^2 \tau_{\omega}^2 \alpha \int [d\mathbf{k}] \mathbf{v} \hat{L} \mathbf{v} \cdot \mathbf{E} f'. \quad (\text{A7})$$

Current that is linear order in scattering time is given by

$$\mathbf{j}_{11}^{(\omega)}(\tau_{\omega}) = e^2 \tau_{\omega} \int [d\mathbf{k}] \left[\xi \mathbf{v}_{\text{m}} \mathbf{E} \cdot \mathbf{v} f' - \eta \mathbf{B} \Omega_{\nu} \mathbf{v} \cdot \mathbf{E} f' - \mathbf{v} (\zeta \Omega_{\nu} \mathbf{B} - \gamma \Omega_{\text{B}} \mathbf{v}) \cdot \mathbf{E} f' + \xi \mathbf{v} \mathbf{E} \cdot (\mathbf{v}_{\text{m}} f' + \epsilon_{\text{m}} \mathbf{v} f'') \right]. \quad (\text{A8})$$

The linear- \mathbf{B} dependent currents calculated in Eqs. (A6)-(A8) have been earlier discussed in Refs. [42, 43, 45, and 73]. In presence of TRS (broken SIS) various quantities satisfy $(\epsilon_{\text{m}}, \boldsymbol{\Omega})(-\mathbf{k}) = -(\epsilon_{\text{m}}, \boldsymbol{\Omega})(\mathbf{k})$, $\mathbf{v}(-\mathbf{k}) = -\mathbf{v}(\mathbf{k})$ and $\mathbf{v}_{\text{m}}(-\mathbf{k}) = \mathbf{v}_{\text{m}}(\mathbf{k})$, hence all the contributions $\propto \tau_{\omega}$ vanish. However, currents proportional to the even power of scattering time survives, out of which the Lorentz force contribution $\propto \tau_{\omega}^2$ gives rise to the classical Hall effect [61 and 74], and the anomalous velocity contribution $\propto \tau_{\omega}^0$ gives rise to OMM induced intrinsic Hall effect [62]. On the other hand, in presence of SIS (broken TRS) the various quantities satisfy $(\epsilon_{\text{m}}, \boldsymbol{\Omega})(-\mathbf{k}) = (\epsilon_{\text{m}}, \boldsymbol{\Omega})(\mathbf{k})$, $\mathbf{v}(-\mathbf{k}) = -\mathbf{v}(\mathbf{k})$, $\mathbf{v}_{\text{m}}(-\mathbf{k}) = -\mathbf{v}_{\text{m}}(\mathbf{k})$, and in that case all the linear- \mathbf{B} dependent terms are expected to be non-zero.

Appendix B: Semiclassical theory for the nonlinear conductivities

In this section of Appendix, we calculate current that is NL in \mathbf{E} -field. The ansatz for the non-equilibrium part of the distribution function quadratic in \mathbf{E} -field [33 and 43] can be written as

$$f_2(t) = f_2^{(0)} + f_2^{(0)*} + f_2^{(2\omega)} e^{i2\omega t} + f_2^{(2\omega)*} e^{-i2\omega t}, \quad (\text{B1})$$

where $f_2^{(0)}$ represents the rectification part and $f_2^{(2\omega)}$ represents the second harmonic part. With this, from Eq. (3) we obtain

$$f_2^{(2\omega)} = \sum_{\nu} \left(\alpha D \tau_{2\omega} \hat{L} \right)^{\nu} D \frac{e\tau_{2\omega}}{\hbar} \left[\mathbf{E} + \zeta \frac{e}{\hbar} (\mathbf{E} \cdot \mathbf{B}) \boldsymbol{\Omega} \right] \cdot \nabla_{\mathbf{k}} f_1^{(\omega)}, \quad (\text{B2})$$

and

$$f_2^{(0)} = \sum_{\nu} \left(\alpha D \tau \hat{L} \right)^{\nu} D \frac{e\tau}{\hbar} \left[\mathbf{E}^* + \zeta \frac{e}{\hbar} (\mathbf{E}^* \cdot \mathbf{B}) \boldsymbol{\Omega} \right] \cdot \nabla_{\mathbf{k}} f_1^{(\omega)}. \quad (\text{B3})$$

We emphasize that from Eq. (B2) we can generate Eq. (B3) by $\tau_{2\omega} \rightarrow \tau$ and $\mathbf{E} \rightarrow \mathbf{E}^*$. From this master solution it is now straightforward to separate out the distribution function in various order in magnetic field as $f_2^{(2\omega)} = f_{20}^{(2\omega)} + f_{21}^{(2\omega)}$. These can be calculated as

$$f_{20}^{(2\omega)}(\tau_{2\omega}, \tau_{\omega}) = \frac{e^2 \tau_{2\omega} \tau_{\omega}}{\hbar} (\mathbf{E} \cdot \nabla_{\mathbf{k}}) \mathbf{E} \cdot \mathbf{v} f', \quad (\text{B4})$$

$$f_{21}^{(2\omega)}(\tau_{2\omega}, \tau_{\omega}) = \frac{e^2 \tau_{2\omega} \tau_{\omega}}{\hbar} \left[\zeta \frac{e}{\hbar} (\mathbf{E} \cdot \mathbf{B}) (\boldsymbol{\Omega} \cdot \nabla_{\mathbf{k}}) \mathbf{v} \cdot \mathbf{E} f' - \gamma \Omega_{\text{B}} (\mathbf{E} \cdot \nabla_{\mathbf{k}}) \mathbf{v} \cdot \mathbf{E} f' + (\mathbf{E} \cdot \nabla_{\mathbf{k}}) \{ (\zeta \Omega_{\text{v}} \mathbf{B} - \gamma \Omega_{\text{B}} \mathbf{v}) \cdot \mathbf{E} f' - \xi \mathbf{E} \cdot (\mathbf{v}_{\text{m}} f' + \epsilon_{\text{m}} \mathbf{v} f'') \} \right], \quad (\text{B5})$$

$$f_{21}^{(2\omega)}(\tau_{2\omega}^2, \tau_{\omega}) = \alpha \frac{e^2 \tau_{2\omega}^2 \tau_{\omega}}{\hbar} \hat{L} (\mathbf{E} \cdot \nabla_{\mathbf{k}}) \mathbf{E} \cdot \mathbf{v} f', \quad f_{21}^{(2\omega)}(\tau_{2\omega}, \tau_{\omega}^2) = \alpha \frac{e^2 \tau_{2\omega} \tau_{\omega}^2}{\hbar} (\mathbf{E} \cdot \nabla_{\mathbf{k}}) \hat{L} \mathbf{v} \cdot \mathbf{E} f'. \quad (\text{B6})$$

We note that the first two expressions are $\propto \tau^2$ and the last two expressions are $\propto \tau^3$. We can obtain the rectification part, $f_2^{(0)}$ from these expressions just by replacing $\tau_{2\omega}$ by τ and \mathbf{E} , first one from the left, by \mathbf{E}^* . These results are consistent with the previous studies [42 and 43].

The magnetic field independent contributions to the current come from the semiclassical band velocity and Berry curvature induced anomalous velocity. The second harmonic current that is zeroth order in magnetic field, can be written as $\mathbf{j}_{20}(t) = \mathbf{j}_{20}^{(2\omega)} e^{i2\omega t} + \mathbf{j}_{20}^{(2\omega)*} e^{-i2\omega t}$ where

$$\mathbf{j}_{20}^{(2\omega)}(\tau_{\omega}) = -\frac{e^3 \tau_{\omega}}{\hbar} \int [d\mathbf{k}] (\mathbf{E} \times \boldsymbol{\Omega}) \mathbf{v} \cdot \mathbf{E} f', \quad (\text{B7})$$

$$\mathbf{j}_{20}^{(2\omega)}(\tau_{\omega}, \tau_{2\omega}) = -\frac{e^3 \tau_{\omega} \tau_{2\omega}}{\hbar} \int [d\mathbf{k}] \mathbf{v} (\mathbf{E} \cdot \nabla_{\mathbf{k}}) \mathbf{E} \cdot \mathbf{v} f'. \quad (\text{B8})$$

The rectification part can be written as $\mathbf{j}_{20} = \mathbf{j}_{20} + \mathbf{j}_{20}^*$ replacing $\tau_{2\omega}$ by τ and \mathbf{E} (first one from the left) by \mathbf{E}^* in the above expressions. The $\mathbf{j}_{20}^{(2\omega)}(\tau_{\omega})$ represents the NL anomalous current [35 and 53] while the second term is the ordinary NL Drude current originating from the band velocity. In presence of TRS but broken SIS, only the NL anomalous Hall contribution is expected to be non-zero. The breaking of SIS plays the key role in the quadratic NL response, as in presence of SIS both the contributions vanish identically.

For the linear- \mathbf{B} contributions, the second harmonic current can be similarly written as $\mathbf{j}_{21}(t) = \mathbf{j}_{21}^{(2\omega)} e^{i2\omega t} + \mathbf{j}_{21}^{(2\omega)*} e^{-i2\omega t}$. In various orders of scattering time we obtain

$$\mathbf{j}_{21}^{(2\omega)}(\tau_{\omega}) = -\frac{e^3 \tau_{\omega}}{\hbar} \int [d\mathbf{k}] (\mathbf{E} \times \boldsymbol{\Omega}) [(\zeta \Omega_{\text{v}} \mathbf{B} - \gamma \Omega_{\text{B}} \mathbf{v}) \cdot \mathbf{E} f' - \xi \mathbf{E} \cdot (\mathbf{v}_{\text{m}} f' + \epsilon_{\text{m}} \mathbf{v} f'')], \quad (\text{B9})$$

$$\mathbf{j}_{21}^{(2\omega)}(\tau_{\omega}^2) = -\alpha \frac{e^3 \tau_{\omega}^2}{\hbar} \int [d\mathbf{k}] (\mathbf{E} \times \boldsymbol{\Omega}) \hat{L} \mathbf{v} \cdot \mathbf{E} f', \quad (\text{B10})$$

$$\mathbf{j}_{21}^{(2\omega)}(\tau_{\omega}, \tau_{2\omega}) = -\frac{e^3 \tau_{\omega} \tau_{2\omega}}{\hbar} \int [d\mathbf{k}] (\eta \Omega_{\text{v}} \mathbf{B} - \xi \mathbf{v}_{\text{m}}) (\mathbf{E} \cdot \nabla_{\mathbf{k}}) \mathbf{v} \cdot \mathbf{E} f' - \frac{e^3 \tau_{\omega} \tau_{2\omega}}{\hbar} \int [d\mathbf{k}] \mathbf{v} \left[\zeta \frac{e}{\hbar} (\mathbf{E} \cdot \mathbf{B}) (\boldsymbol{\Omega} \cdot \nabla_{\mathbf{k}}) \mathbf{v} \cdot \mathbf{E} f' - \gamma \Omega_{\text{B}} (\mathbf{E} \cdot \nabla_{\mathbf{k}}) \mathbf{v} \cdot \mathbf{E} f' + (\mathbf{E} \cdot \nabla_{\mathbf{k}}) [(\zeta \Omega_{\text{v}} \mathbf{B} - \gamma \Omega_{\text{B}} \mathbf{v}) \cdot \mathbf{E} f' - \xi \mathbf{E} \cdot (\mathbf{v}_{\text{m}} f' + \epsilon_{\text{m}} \mathbf{v} f'')] \right], \quad (\text{B11})$$

$$\mathbf{j}_{21}^{(2\omega)}(\tau_{\omega}, \tau_{2\omega}^2) = -\alpha \frac{e^3 \tau_{\omega} \tau_{2\omega}^2}{\hbar} \int [d\mathbf{k}] \mathbf{v} \hat{L} (\mathbf{E} \cdot \nabla_{\mathbf{k}}) \mathbf{v} \cdot \mathbf{E} f', \quad \mathbf{j}_{21}^{(2\omega)}(\tau_{\omega}^2, \tau_{2\omega}) = -\alpha \frac{e^3 \tau_{2\omega} \tau_{\omega}^2}{\hbar} \int [d\mathbf{k}] \mathbf{v} (\mathbf{E} \cdot \nabla_{\mathbf{k}}) \hat{L} \mathbf{v} \cdot \mathbf{E} f'. \quad (\text{B12})$$

The NL conductivities extracted from these expressions are presented in the main text. We note that this general formalism for linear \mathbf{B} -field dependent NL conductivity has been earlier discussed in Refs. [42 and 43]. It is straightforward to see that in presence of SIS (TRS broken), all these terms vanish identically. In presence of TRS (broken SIS) however the current $\propto \tau^2$ survives while the contributions $\propto (\tau, \tau^3)$ vanish identically.

Appendix C: Details of calculation for nonlinear conductivity in WSM

In this section of Appendix, we present the details of our calculation of NL conductivity for a pair of Weyl nodes of which one is situated at energy Q_0 and the other is situated at energy $-Q_0$. For that we first calculate the NL conductivities of a single Weyl node with band crossing at zero energy given by $H_s(\mathbf{k}) = s\hbar v_F \boldsymbol{\sigma} \cdot \mathbf{k}$. Then we modify the Fermi energy dependences for individual nodes to include the posi-

tional shift in the energy. The velocity for this model Hamiltonian is given by $\mathbf{v} = s_{\text{b}} v_F \mathbf{k}/k$, while the Berry curvature and OMM are given by [43 and 50] $\boldsymbol{\Omega} = -s s_{\text{b}} \mathbf{k}/(2k^3)$ and $\mathbf{m} = -s e v_F \mathbf{k}/(2k^2)$. The linear Drude conductivities which are diagonal components of the linear conductivity matrix in absence of magnetic field are calculated to be [72]

$$\sigma_{aa} = \frac{e^2 \tau \mu^2}{6\pi^2 \hbar^3 v_F}; \quad a \in (x, y, z). \quad (\text{C1})$$

Equation (C1) does not depend on the chirality of the nodes and whether the Fermi levels reside in the conduction band or valence band. In presence of magnetic field the Onsager's reciprocal relations restrict the longitudinal conductivities to be minimum quadratic order in magnetic field which is out of the scope of this paper. However, the off-diagonal components can have minimum linear- \mathbf{B} dependence and are obtained to be [62]

$$\sigma_{ab} = -\varepsilon_{abc} B_c \frac{s_{\text{b}} e^3 v_F}{24\pi^2 \hbar^3 |\mu|} (\xi \hbar^2 + 4\alpha \tau^2 \mu^2). \quad (\text{C2})$$

σ_{abc}	σ_{axx}	σ_{axy}	σ_{axz}	σ_{ayx}	σ_{ayy}	σ_{ayz}	σ_{azz}	σ_{azy}	σ_{azz}
σ_{xbc}	$(-2\eta + 2\zeta)B_x$	$(-\gamma + 2\zeta)B_y$	$(-\gamma + 2\zeta)B_z$	αB_y	$(-2\eta - \alpha + \gamma)B_x$	$-s_b \frac{\sigma_0}{\chi_0}$	$-\alpha B_z$	$-s_b \frac{\sigma_0}{\chi_0}$	$(-2\eta + \alpha + \gamma)B_x$
σ_{ybc}	$(-2\eta + \alpha + \gamma)B_y$	$-\alpha B_x$	$-s_b \frac{\sigma_0}{\chi_0}$	$(-\gamma + 2\zeta)B_x$	$(-2\eta + 2\zeta)B_y$	$(-\gamma + 2\zeta)B_z$	$-s_b \frac{\sigma_0}{\chi_0}$	αB_z	$(-2\eta - \alpha + \gamma)B_y$
σ_{zbc}	$(-2\eta - \alpha + \gamma)B_z$	$-s_b \frac{\sigma_0}{\chi_0}$	αB_x	$-s_b \frac{\sigma_0}{\chi_0}$	$(-2\eta + \alpha + \gamma)B_z$	$-\alpha B_y$	$(-\gamma + 2\zeta)B_x$	$(-\gamma + 2\zeta)B_y$	$(-2\eta + 2\zeta)B_z$

TABLE II. Nonlinear conductivity elements (in unit of $ss_b\chi_0/12$) for a single node of a WSM with band crossing (charge neutrality point) situated at zero energy. Here, we have defined $\chi_0 = e^4\tau^2v_F^2/(\pi^2\hbar^2|\mu|)$ and $\sigma_0 = e^3\tau/(\pi^2\hbar^2)$. Note that we have also included the NL anomalous Hall effect here which are independent of magnetic field.

Note that the OMM and Lorentz force cause the ordinary Hall effect.

The magnetic field independent and linear- \mathbf{B} dependent NL conductivities have been summarized in Table II. We obtain the NL anomalous Hall conductivities to be

$$\sigma_{abc}^{\text{NAH}} = -\varepsilon_{abc} \frac{se^3\tau}{12\pi^2\hbar^2}. \quad (\text{C3})$$

We note that it is independent of chemical potential and depends on the chirality. So even for Weyl nodes separated in energy its total contribution will vanish. The magnetic field dependent NL conductivities originate from various sources and are written in units of

$$\sigma_{\text{NL}}^{\text{S}} = ss_b \frac{\chi_0}{12} \quad \text{with} \quad \chi_0 = \frac{e^4\tau^2v_F^2}{\pi^2\hbar^2|\mu|}. \quad (\text{C4})$$

The various contributions of magnetic field are also highlighted in the table inside the parenthesis. We note that our results for the NL conductivities are consistent with Ref. [43], where the effect of Lorentz force effect was ignored. If we ignore the effect of Lorentz force, then for magnetic field along the \hat{z} the expression of σ_{zxx} matches with the expression given in Ref. [43].

Given the expressions of NL conductivity for Weyl node at zero energy, now we will show how to modify these expressions to obtain results for Weyl nodes separated in energy. We will show this for the Eq. (C4) and the modification in linear conductivities can be obtained following similar steps. For scenario-I shown in Fig. 1(c) we obtain

$$\sigma_{\text{NL}}^{\text{S}}(+1) = \frac{e^4\tau^2v_F^2}{12\pi^2\hbar^2(|\mu| + Q_0)}; \quad \sigma_{\text{NL}}^{\text{S}}(-1) = -\frac{e^4\tau^2v_F^2}{12\pi^2\hbar^2(|\mu| - Q_0)}, \quad (\text{C5})$$

for scenario-III we obtain

$$\sigma_{\text{NL}}^{\text{S}}(+1) = -\frac{e^4\tau^2v_F^2}{12\pi^2\hbar^2(|\mu| - Q_0)}; \quad \sigma_{\text{NL}}^{\text{S}}(-1) = \frac{e^4\tau^2v_F^2}{12\pi^2\hbar^2(|\mu| + Q_0)}, \quad (\text{C6})$$

and for scenario-II we obtain

$$\begin{aligned} \sigma_{\text{NL}}^{\text{S}}(+1) &= \frac{e^4\tau^2v_F^2}{12\pi^2\hbar^2(\pm|\mu| + Q_0)} \\ \sigma_{\text{NL}}^{\text{S}}(-1) &= -\frac{e^4\tau^2v_F^2}{12\pi^2\hbar^2(\pm|\mu| - Q_0)} \end{aligned} \quad (\text{C7})$$

In Eq. (C7) the $+(-)$ sign in the denominator in front of $|\mu|$ corresponds to $\mu > 0(\mu < 0)$ in scenario-II. The total NL conductivities are obtained by adding the contribution from the two nodes. Comparing scenario-I with -III, one can easily identify that

$$\sigma_{\text{NL}}^{\text{S,I}}(+1) = \sigma_{\text{NL}}^{\text{S,III}}(-1), \quad \sigma_{\text{NL}}^{\text{S,I}}(-1) = \sigma_{\text{NL}}^{\text{S,III}}(+1). \quad (\text{C8})$$

So the NL conductivities will be identical in both these cases after summing over the nodes. Similarly, when we compare scenario-I to -II, it can be checked that

$$\begin{aligned} \sigma_{\text{NL}}^{\text{S,I}}(+1) &= \sigma_{\text{NL}}^{\text{S,II}}(+1), \quad \sigma_{\text{NL}}^{\text{S,I}}(-1) = \sigma_{\text{NL}}^{\text{S,II}}(-1) \quad \text{for } \mu > 0, \\ \sigma_{\text{NL}}^{\text{S,I}}(+1) &= \sigma_{\text{NL}}^{\text{S,II}}(-1), \quad \sigma_{\text{NL}}^{\text{S,I}}(-1) = \sigma_{\text{NL}}^{\text{S,II}}(+1) \quad \text{for } \mu < 0. \end{aligned} \quad (\text{C9})$$

So in the above two scenarios also, the NL conductivities turned out to be identical after considering the contributions of all the nodes. In conclusion, the NL conductivities do not depend on the position of the Fermi level.

* dmandal@iitk.ac.in

† kamaldas@iitk.ac.in

‡ amitag@iitk.ac.in

¹ Xiangang Wan, Ari M. Turner, Ashvin Vishwanath, and Sergey Y. Savrasov, "Topological semimetal and fermi-arc surface states in the electronic structure of pyrochlore iridates," *Phys. Rev. B* **83**, 205101 (2011).

² Hongming Weng, Chen Fang, Zhong Fang, B. Andrei Bernevig, and Xi Dai, "Weyl semimetal phase in non-centrosymmetric transition-metal monophosphides," *Phys. Rev. X* **5**, 011029 (2015).

³ B. Q. Lv, H. M. Weng, B. B. Fu, X. P. Wang, H. Miao, J. Ma, P. Richard, X. C. Huang, L. X. Zhao, G. F. Chen, Z. Fang, X. Dai, T. Qian, and H. Ding, "Experimental discovery of weyl semimetal taas," *Phys. Rev. X* **5**, 031013 (2015).

⁴ Su-Yang Xu, Ilya Belopolski, Nasser Alidoust, Madhab Neupane, Guang Bian, Chenglong Zhang, Raman Sankar, Guoqing Chang, Zhujun Yuan, Chi-Cheng Lee, Shin-Ming Huang, Hao Zheng, Jie Ma, Daniel S. Sanchez, BaoKai Wang, Arun Bansil, Fangcheng Chou, Pavel P. Shibayev, Hsin Lin, Shuang Jia, and M. Zahid Hasan, "Discovery

- of a weyl fermion semimetal and topological fermi arcs,” *Science* **349**, 613–617 (2015).
- ⁵ Su-Yang Xu, Ilya Belopolski, Daniel S. Sanchez, Chenglong Zhang, Guoqing Chang, Cheng Guo, Guang Bian, Zhujun Yuan, Hong Lu, Tay-Rong Chang, Pavel P. Shibayev, Mykhailo L. Prokopovych, Nasser Alidoust, Hao Zheng, Chi-Cheng Lee, Shin-Ming Huang, Raman Sankar, Fangcheng Chou, Chuang-Han Hsu, Horng-Tay Jeng, Arun Bansil, Titus Neupert, Vladimir N. Strocov, Hsin Lin, Shuang Jia, and M. Zahid Hasan, “Experimental discovery of a topological weyl semimetal state in tap,” *Science Advances* **1**, e1501092 (2015).
 - ⁶ M. Zahid Hasan, Su-Yang Xu, Ilya Belopolski, and Shin-Ming Huang, “Discovery of weyl fermion semimetals and topological fermi arc states,” *Annual Review of Condensed Matter Physics* **8**, 289–309 (2017).
 - ⁷ Binghai Yan and Claudia Felser, “Topological materials: Weyl semimetals,” *Annual Review of Condensed Matter Physics* **8**, 337–354 (2017).
 - ⁸ N. P. Armitage, E. J. Mele, and Ashvin Vishwanath, “Weyl and dirac semimetals in three-dimensional solids,” *Rev. Mod. Phys.* **90**, 015001 (2018).
 - ⁹ B. Q. Lv, T. Qian, and H. Ding, “Experimental perspective on three-dimensional topological semimetals,” *Rev. Mod. Phys.* **93**, 025002 (2021).
 - ¹⁰ Maxim N. Chernodub, Yago Ferreira, Adolfo G. Grushin, Karl Landsteiner, and María A. H. Vozmediano, “Thermal transport, geometry, and anomalies,” (2021), [arXiv:2110.05471 \[cond-mat.mes-hall\]](https://arxiv.org/abs/2110.05471).
 - ¹¹ Shinichi Nishihaya, Masaki Uchida, Yusuke Nakazawa, Ryosuke Kurihara, Kazuto Akiba, Markus Kriener, Atsushi Miyake, Yasujiro Taguchi, Masashi Tokunaga, and Masashi Kawasaki, “Quantized surface transport in topological dirac semimetal films,” *Nature Communications* **10**, 2564 (2019).
 - ¹² Shinichi Nishihaya, Masaki Uchida, Yusuke Nakazawa, Markus Kriener, Yasujiro Taguchi, and Masashi Kawasaki, “Intrinsic coupling between spatially-separated surface fermi-arcs in weyl orbit quantum hall states,” *Nature Communications* **12**, 2572 (2021).
 - ¹³ H. Sagayama, D. Uematsu, T. Arima, K. Sugimoto, J. J. Ishikawa, E. O’Farrell, and S. Nakatsuji, “Determination of long-range all-in-all-out ordering of ir^{4+} moments in a pyrochlore iridate $eu_2ir_2o_7$ by resonant x-ray diffraction,” *Phys. Rev. B* **87**, 100403 (2013).
 - ¹⁴ Steven M. Disseler, “Direct evidence for the all-in/all-out magnetic structure in the pyrochlore iridates from muon spin relaxation,” *Phys. Rev. B* **89**, 140413 (2014).
 - ¹⁵ Zhijun Wang, Hongming Weng, Quansheng Wu, Xi Dai, and Zhong Fang, “Three-dimensional dirac semimetal and quantum transport in cd_3as_2 ,” *Phys. Rev. B* **88**, 125427 (2013).
 - ¹⁶ Zhijun Wang, Yan Sun, Xing-Qiu Chen, Cesare Franchini, Gang Xu, Hongming Weng, Xi Dai, and Zhong Fang, “Dirac semimetal and topological phase transitions in A_3bi ($a = Na, k, rb$),” *Phys. Rev. B* **85**, 195320 (2012).
 - ¹⁷ Shin-Ming Huang, Su-Yang Xu, Ilya Belopolski, Chi-Cheng Lee, Guoqing Chang, BaoKai Wang, Nasser Alidoust, Guang Bian, Madhab Neupane, Chenglong Zhang, Shuang Jia, Arun Bansil, Hsin Lin, and M. Zahid Hasan, “A weyl fermion semimetal with surface fermi arcs in the transition metal monopnictide taas class,” *Nature Communications* **6**, 7373 (2015).
 - ¹⁸ A. A. Zyuzin, Si Wu, and A. A. Burkov, “Weyl semimetal with broken time reversal and inversion symmetries,” *Phys. Rev. B* **85**, 165110 (2012).
 - ¹⁹ Guoqing Chang, Bahadur Singh, Su-Yang Xu, Guang Bian, Shin-Ming Huang, Chuang-Han Hsu, Ilya Belopolski, Nasser Alidoust, Daniel S. Sanchez, Hao Zheng, Hong Lu, Xiao Zhang, Yi Bian, Tay-Rong Chang, Horng-Tay Jeng, Arun Bansil, Han Hsu, Shuang Jia, Titus Neupert, Hsin Lin, and M. Zahid Hasan, “Magnetic and noncentrosymmetric weyl fermion semimetals in the $RAI\text{Ge}$ family of compounds ($R = \text{rare earth}$),” *Phys. Rev. B* **97**, 041104 (2018).
 - ²⁰ Hung-Yu Yang, Bahadur Singh, Jonathan Gaudet, Baozhu Lu, Cheng-Yi Huang, Wei-Chi Chiu, Shin-Ming Huang, Baokai Wang, Faranak Bahrami, Bochao Xu, Jacob Franklin, Ilya Sochnikov, David E. Graf, Guangyong Xu, Yang Zhao, Christina M. Hoffman, Hsin Lin, Darius H. Torchinsky, Collin L. Broholm, Arun Bansil, and Fazel Tafti, “Noncollinear ferromagnetic weyl semimetal with anisotropic anomalous hall effect,” *Phys. Rev. B* **103**, 115143 (2021).
 - ²¹ Robert Boyd, *Nonlinear optics* (Academic Press, Amsterdam Boston, 2008).
 - ²² J. Orenstein, J.E. Moore, T. Morimoto, D.H. Torchinsky, J.W. Harter, and D. Hsieh, “Topology and symmetry of quantum materials via nonlinear optical responses,” *Annual Review of Condensed Matter Physics* **12**, 247–272 (2021).
 - ²³ Sanjib Kumar Das, Tanay Nag, and Snehasish Nandy, “Topological magnus responses in two- and three-dimensional systems,” *Phys. Rev. B* **104**, 115420 (2021).
 - ²⁴ Ching-Kit Chan, Netanel H. Lindner, Gil Refael, and Patrick A. Lee, “Photocurrents in weyl semimetals,” *Phys. Rev. B* **95**, 041104 (2017).
 - ²⁵ Fernando de Juan, Adolfo G. Grushin, Takahiro Morimoto, and Joel E. Moore, “Quantized circular photogalvanic effect in weyl semimetals,” *Nature Communications* **8**, 15995 (2017).
 - ²⁶ L. E. Golub, E. L. Ivchenko, and B. Z. Spivak, “Photocurrent in gyrotropic weyl semimetals,” *JETP Letters* **105**, 782–785 (2017).
 - ²⁷ Dmitri E. Kharzeev, Yuta Kikuchi, René Meyer, and Yuya Tanizaki, “Giant photocurrent in asymmetric weyl semimetals from the helical magnetic effect,” *Phys. Rev. B* **98**, 014305 (2018).
 - ²⁸ L. E. Golub and E. L. Ivchenko, “Circular and magnetoinduced photocurrents in weyl semimetals,” *Phys. Rev. B* **98**, 075305 (2018).
 - ²⁹ Daniel E. Parker, Takahiro Morimoto, Joseph Orenstein, and Joel E. Moore, “Diagrammatic approach to nonlinear optical response with application to weyl semimetals,” *Phys. Rev. B* **99**, 045121 (2019).
 - ³⁰ Banasree Sadhukhan and Tanay Nag, “Role of time reversal symmetry and tilting in circular photogalvanic responses,” *Phys. Rev. B* **103**, 144308 (2021).
 - ³¹ Banasree Sadhukhan and Tanay Nag, “Electronic structure and unconventional nonlinear response in double weyl semimetal $Srsi_2$,” *Phys. Rev. B* **104**, 245122 (2021).
 - ³² Jing Li, Tian Xu, Guo-Bao Zhu, and Hui Pan, “Photoinduced anomalous hall and nonlinear hall effect in borophene,” *Solid State Communications* **322**, 114092 (2020).
 - ³³ E. Deyo, L. E. Golub, E. L. Ivchenko, and B. Spivak, “Semiclassical theory of the photogalvanic effect in noncentrosymmetric systems,” (2009), [arXiv:0904.1917 \[cond-](https://arxiv.org/abs/0904.1917)

- mat.mes-hall].
- 34 J. E. Moore and J. Orenstein, “Confinement-induced berry phase and helicity-dependent photocurrents,” *Phys. Rev. Lett.* **105**, 026805 (2010).
 - 35 Inti Sodemann and Liang Fu, “Quantum nonlinear hall effect induced by berry curvature dipole in time-reversal invariant materials,” *Phys. Rev. Lett.* **115**, 216806 (2015).
 - 36 Qiong Ma, Su-Yang Xu, Huitao Shen, David MacNeill, Valla Fatemi, Tay-Rong Chang, Andrés M. Mier Valdivia, Sanfeng Wu, Zongzheng Du, Chuang-Han Hsu, Shiang Fang, Quinn D. Gibson, Kenji Watanabe, Takashi Taniguchi, Robert J. Cava, Efthimios Kaxiras, Hai-Zhou Lu, Hsin Lin, Liang Fu, Nuh Gedik, and Pablo Jarillo-Herrero, “Observation of the nonlinear hall effect under time-reversal-symmetric conditions,” *Nature* **565**, 337–342 (2019).
 - 37 Z. Z. Du, Hai-Zhou Lu, and X. C. Xie, “Nonlinear hall effects,” *Nature Reviews Physics* (2021), 10.1038/s42254-021-00359-6.
 - 38 Carmine Ortix, “Nonlinear hall effect with time-reversal symmetry: Theory and material realizations,” *Advanced Quantum Technologies* **4**, 2100056 (2021).
 - 39 E. J. König, H.-Y. Xie, D. A. Pesin, and A. Levchenko, “Photogalvanic effect in weyl semimetals,” *Phys. Rev. B* **96**, 075123 (2017).
 - 40 Habib Rostami and Marco Polini, “Nonlinear anomalous photocurrents in weyl semimetals,” *Phys. Rev. B* **97**, 195151 (2018).
 - 41 Chuanchang Zeng, Snehasish Nandy, and Sumanta Tewari, “Nonlinear transport in weyl semimetals induced by berry curvature dipole,” *Phys. Rev. B* **103**, 245119 (2021).
 - 42 Alberto Cortijo, “Magnetic-field-induced nonlinear optical responses in inversion symmetric dirac semimetals,” *Phys. Rev. B* **94**, 235123 (2016).
 - 43 Takahiro Morimoto, Shudan Zhong, Joseph Orenstein, and Joel E. Moore, “Semiclassical theory of nonlinear magneto-optical responses with applications to topological dirac/weyl semimetals,” *Phys. Rev. B* **94**, 245121 (2016).
 - 44 Snehasish Nandy, Chuanchang Zeng, and Sumanta Tewari, “Chiral anomaly induced nonlinear hall effect in multi-weyl semimetals,” (2021), arXiv:2104.14969 [cond-mat.mes-hall].
 - 45 Yang Gao, “Semiclassical dynamics and nonlinear charge current,” *Frontiers of Physics* **14**, 33404 (2019).
 - 46 E. V. Gorbar, V. A. Miransky, I. A. Shovkovy, and P. O. Sukhachov, “Second-order chiral kinetic theory: Chiral magnetic and pseudomagnetic waves,” *Phys. Rev. B* **95**, 205141 (2017).
 - 47 L. E. Golub, E. L. Ivchenko, and B. Spivak, “Semiclassical theory of the circular photogalvanic effect in gyrotropic systems,” *Phys. Rev. B* **102**, 085202 (2020).
 - 48 Vladimir A. Zyuzin, “Chiral electric separation effect in weyl semimetals,” *Phys. Rev. B* **98**, 165205 (2018).
 - 49 Alexander A. Zyuzin, Mihail Silaev, and Vladimir A. Zyuzin, “Nonlinear chiral transport in dirac semimetals,” *Phys. Rev. B* **98**, 205149 (2018).
 - 50 Rui-Hao Li, Olle G. Heinonen, Anton A. Burkov, and Steven S.-L. Zhang, “Nonlinear hall effect in weyl semimetals induced by chiral anomaly,” *Phys. Rev. B* **103**, 045105 (2021).
 - 51 Pan He, Steven S.-L. Zhang, Dapeng Zhu, Shuyuan Shi, Olle G. Heinonen, Giovanni Vignale, and Hyunsoo Yang, “Nonlinear planar hall effect,” *Phys. Rev. Lett.* **123**, 016801 (2019).
 - 52 Giulia Pacchioni, “The hall effect goes nonlinear,” *Nature Reviews Materials* **4**, 514–514 (2019).
 - 53 Kaifei Kang, Tingxin Li, Egon Sohn, Jie Shan, and Kin Fai Mak, “Nonlinear anomalous hall effect in few-layer wte2,” *Nature Materials* **18**, 324–328 (2019).
 - 54 O. O. Shvetsov, V. D. Esin, A. V. Timonina, N. N. Kolesnikov, and E. V. Deviatov, “Nonlinear hall effect in three-dimensional weyl and dirac semimetals,” *JETP Letters* **109**, 715–721 (2019).
 - 55 Ming-Che Chang and Qian Niu, “Berry phase, hyperorbits, and the hofstadter spectrum,” *Phys. Rev. Lett.* **75**, 1348–1351 (1995).
 - 56 Ganesh Sundaram and Qian Niu, “Wave-packet dynamics in slowly perturbed crystals: Gradient corrections and berry-phase effects,” *Phys. Rev. B* **59**, 14915–14925 (1999).
 - 57 Yang Gao, Shengyuan A. Yang, and Qian Niu, “Field induced positional shift of bloch electrons and its dynamical implications,” *Phys. Rev. Lett.* **112**, 166601 (2014).
 - 58 Yang Gao, Shengyuan A. Yang, and Qian Niu, “Geometrical effects in orbital magnetic susceptibility,” *Phys. Rev. B* **91**, 214405 (2015).
 - 59 N.W. Ashcroft and N.D. Mermin, *Solid State Physics*, HRW international editions (Holt, Rinehart and Winston, 1976).
 - 60 Takahiro Morimoto and Naoto Nagaosa, “Scaling laws for nonlinear electromagnetic responses of dirac fermion,” *Phys. Rev. B* **93**, 125125 (2016).
 - 61 C. M. Hurd, *The Hall effect in metals and alloys* (Plenum Press, New York, 1972).
 - 62 Kamal Das and Amit Agarwal, “Intrinsic hall conductivities induced by the orbital magnetic moment,” *Phys. Rev. B* **103**, 125432 (2021).
 - 63 H.B. Nielsen and Masao Ninomiya, “The adler-bell-jackiw anomaly and weyl fermions in a crystal,” *Physics Letters B* **130**, 389–396 (1983).
 - 64 Shuichi Murakami, “Phase transition between the quantum spin hall and insulator phases in 3d: emergence of a topological gapless phase,” *New Journal of Physics* **9**, 356–356 (2007).
 - 65 Ilya Belopolski, Peng Yu, Daniel S. Sanchez, Yukiaki Ishida, Tay-Rong Chang, Songtian S. Zhang, Su-Yang Xu, Hao Zheng, Guoqing Chang, Guang Bian, Horng-Tay Jeng, Takeshi Kondo, Hsin Lin, Zheng Liu, Shik Shin, and M. Zahid Hasan, “Signatures of a time-reversal symmetric weyl semimetal with only four weyl points,” *Nature Communications* **8**, 942 (2017).
 - 66 M. M. Vazifeh and M. Franz, “Electromagnetic response of weyl semimetals,” *Phys. Rev. Lett.* **111**, 027201 (2013).
 - 67 Hao-Ran Chang, Jianhui Zhou, Shi-Xiong Wang, Wen-Yu Shan, and Di Xiao, “Rkky interaction of magnetic impurities in dirac and weyl semimetals,” *Phys. Rev. B* **92**, 241103 (2015).
 - 68 C. J. Tabert, J. P. Carbotte, and E. J. Nicol, “Optical and transport properties in three-dimensional dirac and weyl semimetals,” *Phys. Rev. B* **93**, 085426 (2016).
 - 69 S P Mukherjee and J P Carbotte, “Anomalous DC hall response in noncentrosymmetric tilted weyl semimetals,” *Journal of Physics: Condensed Matter* **30**, 115702 (2018).
 - 70 Jorge I. Facio, Dmitri Efremov, Klaus Koepernik, Jih-Shih You, Inti Sodemann, and Jeroen van den Brink, “Strongly enhanced berry dipole at topological phase transitions in bteit,” *Phys. Rev. Lett.* **121**, 246403 (2018).
 - 71 O. Matsyshyn and I. Sodemann, “Nonlinear hall accelera-

- tion and the quantum rectification sum rule,” [Phys. Rev. Lett. **123**, 246602 \(2019\)](#).
- ⁷² Kamal Das and Amit Agarwal, “Linear magnetochiral transport in tilted type-i and type-ii weyl semimetals,” [Phys. Rev. B **99**, 085405 \(2019\)](#).
- ⁷³ Kamal Das and Amit Agarwal, “Berry curvature induced thermopower in type-i and type-ii weyl semimetals,” [Phys. Rev. B **100**, 085406 \(2019\)](#).
- ⁷⁴ J. M. Ziman, *Principles of the theory of solids* (Cambridge University Press, Cambridge, 1972).